An n-bit adder realized via coherent optical parallel computing

1st Bogdan Reznychenko
Probayes
Grenoble, France
bodgan.reznychenko@probayes.com

2nd Ariela Donval
Elbit Systems
Jerusalem, Israel
ariela.donval@elbitsystems.com

3rd Barbara Fresch
University of Padova
Padova, Italy
barbara.fresch@unipd.it

4th Carlo Nazareno
Institute for Physical and Chemical Processes
Bari, Italy
carlonazareno@libero.it

5th Dimitar Dimitrov
Probayes
Grenoble, France
dimitar.dimitrov@probayes.com

6th Elisabetta Collini
University of Padova
Padova, Italy
elisabetta.collini@unipd.it

7th Emmanuel Mazer
Probayes
Grenoble, France
emazer@probayes.com

8th Francoise Remacle
University of Liege
Liège, Belgium
FRemacle@uliege.be

9th Hugo Gattuso
University of Liège
Liège, Belgium
hgattuso@uliege.be

10th Marinella Striccoli
Institute for Physical and Chemical Processes
Bari, Italy
m.striccoli@ba.ipcf.cnr.it

11th Maurizio Coden
University of Padova
Padova, Italy
maurizio.coden@unipd.it

12th Noam Gross
Elbit Systems
Jerusalem, Israel
noam.gross@elbitsystems.com

13th Raphael Levine
Hebrew University of Jerusalem
Jerusalem, Israel
rafi@fh.huji.ac.il

14th Yossi Paltiel
Hebrew University of Jerusalem
Jerusalem, Israel
paltiel@mail.huji.ac.il

***Abstract*—The quantum properties of nanosystems present a new opportunity to enhance the power of classical computers, both for the parallelism of the computation and the speed of the optical operations. In this paper we present the COPAC project aiming at development of a ground-breaking nonlinear coherent spectroscopy combining optical addressing and spatially macroscopically resolved optical readout. The discrete structure of transitions between quantum levels provides a basis for implementation of logic functions even at room temperature. Exploiting the superposition of quantum states gives rise to the possibility of parallel computation by encoding different input values into transition frequencies. As an example of parallel single instruction multiple data calculation by a device developed during the COPAC project, we present a n-bit adder, showing that due to the properties of the system, the delay of this fundamental circuit can be reduced.**

***Index Terms*—parallel, quantum optical computing**

I. Introduction

There has been much effort recently to create classical logic units exploiting quantum properties of matter [1]. We present here the Coherent Optical parallel computing (COPAC) project, that is a transformative novel area in computing both because of the technology, coherent information transfer by ultrafast laser addressing of engineered quantum dots arrays and because of the specialized parallel processing of large amounts of information.

Funding: EC FET open H2020 project COPAC (#766563).

Since 2001, the group at ULiege[1] and the HUJI[2] groups have developed and demonstrated that complex logic operations can be implemented at the molecular- and nanoscale by exploiting and controlling the dynamics of the response of the internal degrees of freedom of confined systems to various inputs: optical, chemical and electrical [2]–[4].

Partners involved in COPAC already collaborated in demonstrating logic processing by coherent optical addressing by a sequence of three laser pulses on dyes tethered on DNA in a 2D photon echo set-up [5], [6].

As the COPAC project aims at designing a real mahine, the IPCF[3] is in charge of the synthesis of semiconductor quantum dots in quantum confinement regime (as CdSe) with electronic transitions in the visible range (from 530 to 650 nm, according to QD size) to achieve nanostructure with control on the size, shape and crystallinity [7]. These QDs are used by UNIPD[4] to provide 2D photon echo measures which could in turn be interpreted thanks to theoretical models developed in collaboration with ULiege and HUJI [4]. This experiments are conducted on solutions and films. These last medium is provided by HUJI [8], [9]. Finally Elbit and ProbaYes are

[1]The University of Liège, Belgium
[2]The Hebrew University of Jerusalem, Israel
[3]Institute for chemical and physical processes, Italy
[4]The University of Padua, Italy

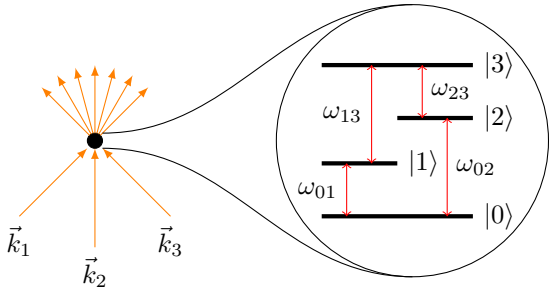

Fig. 1. Scheme of the experiment and the energy levels

respectively in charge of the packaging of the machine and its programming.

The goal of this paper is to give an example how to speed classical computations by taking advantage of the intrinsic parallelism of the device we are building. The particularly interesting example of a circuit to implement is a n-bit adder. In classical logic it is challenging due to long delay times, arising from the necessity to evaluate sums of each pair of bits consecutively. The implementation of 8-bit adder no bigger then 50 nanometers in any dimension even became a subject of Feynman Grand Challenge [10].

In the Sect II of the present paper we briefly describe the idea behind the device able to evaluate binary n-input functions in parallel (the COPAC device in following). In the Sect III follows the description of implementation of logical functions with a device. In Sect IV we present the realization of a parallel n-bit adder with a COPAC device.

II. Physical description

In the present section we provide a description of the method of the calculation with molecular logical units, developed in [4], [5], [11].

A. Language of quantum physics

The states $|x\rangle$ are vectors in Hilbert space. Ket vectors $|x\rangle$ are column vectors, bra vectors $\langle x|$ are row vectors. They relate as $\langle x| = (|x\rangle^*)^T := (|x\rangle)^\dagger$ where † operation is Hermitian conjugation. A scalar product of two vectors is written as $\langle x|y\rangle$.

The operators O that will be used are Hermitian: $O^\dagger = O$. An expectation value of an operator writes $\langle x|O|x\rangle$. It's a quantity that is measured in an experiment.

B. System description

The physical system under study is the one studied in detail in [4]. The energy structure is presented in Fig. 1, where the eigenstates $|i\rangle, i = 0, 1, 2, 3$, are represented as black horizontal lines, and the allowed transitions with their respective frequencies are depicted as red vertical lines. For simplicity we assume that the transition between $|1\rangle$ and $|2\rangle$ is forbidden.

The ensemble of systems is excited by three laser pulses. Each of the pulses has a different propagation direction $\vec{k}_i, i = 1, 2, 3$. The pulses are assumed to either correspond to a single transition frequency or to be spectrally broad, so that they can equally interact with all the transitions of the system.

Due to the large number of systems in the ensemble, there is no need to repeat the experiment multiple times and to average over the results, as the measurement over an ensemble already presents an averaged result [4], [11].

For simplicity we assume that there is no dissipation. The state of the system in this case is represented by a state vector

$$|\phi(t)\rangle = \sum_{j=0}^{3} C_j(t)\,|j\rangle$$

where the $C_j(t)$ coefficients are probability amplitudes, i.e. the probability to find the system in a state $|j\rangle$ at time t is equal to $|C_j(t)|^2$.

The dynamics of the system is described by the Schrödinger equation:

$$\frac{d}{dt}\,|\phi(t)\rangle = -\frac{i}{\hbar}H(t)\,|\phi(t)\rangle \tag{1}$$

where $H(t)$ is the Hamiltonian of the system and $\hbar$ is Planck's constant.

The Hamiltonian $H(t)$ consists of two parts:

$$H(t) = H_0 + V(t) \tag{2}$$

the behavior of the system in absence of the excitation is described by H_0 and the interaction with the light – by $V(t)$. The latter writes $V(t) = \mu E(t)$, where μ is the transition dipole operator and the electric field $E(t)$ is the sum over the three pulses:

$$E(t) = \sum_{j=1}^{3}\left(E_j(t)e^{-i\omega_j t + i\vec{k}_j\vec{r}} + \text{c.c.}\right) \tag{3}$$

The shapes of the pulses are defined by $E_j(t)$. We assume the impulsive limit, with the duration of the pulses much shorter then characteristic times of the system.

To simplify further calculations we use the interaction picture. The operators and the states write respectively:

$$O^I(t) = \exp\left(\frac{i}{\hbar}H_0\,(t-t_0)\right)O(t)\exp\left(-\frac{i}{\hbar}H_0\,(t-t_0)\right) \tag{4}$$

$$|\psi^I(t)\rangle = \exp\left(\frac{i}{\hbar}H_0\,(t-t_0)\right)|\psi(t)\rangle \tag{5}$$

The Schrödinger equation is simplified to

$$\frac{d}{dt}\,|\phi^I(t)\rangle = -\frac{i}{\hbar}V(t)\,|\phi^I(t)\rangle \tag{6}$$

By integration of both right- and left-hand sides, it can be rewritten in a form of an integral equation

$$|\phi^I(t)\rangle = |\phi^I(t_0)\rangle - \frac{i}{\hbar}\int_{t_0}^{t} dt_1\,V(t_1)\,|\phi^I(t_1)\rangle \tag{7}$$

To solve it, we follow [12], iteratively substituting $|\phi^I(t_1)\rangle$ in the right-hand side by the whole right-hand

side $\left(\left|\phi^I(t_0)\right\rangle - \frac{i}{\hbar}\int_{t_0}^{t_{j+1}} dt_j\, V(t_j)\right)$. The right-hand side and thereby the solution of (7) becomes a series of nth order perturbations:

$$\left|\phi^I(t)\right\rangle = \sum_{n=0}^{\infty}\left|\phi^{(n)}(t)\right\rangle \quad (8)$$

$$\left|\phi^{(n)}(t)\right\rangle = \left(-\frac{i}{\hbar}\right)^n \prod_{j=1}^{n}\int_{t_0}^{t_{j+1}} dt_j V(t_j)\left|\phi^I(t_0)\right\rangle \quad (9)$$

where $t_{n+1} = t$ and $\left|\phi^{(0)}(t)\right\rangle = \left|\phi^I(t_0)\right\rangle$.

Note that the nth order perturbation includes n interactions with the electromagnetic field of the pulses.

C. Third-order polarization

The detector of the experimental setup measures the optical response $P(t)$, defined as

$$P(t) = \langle\phi(t)|\,\mu\,|\phi(t)\rangle = \left\langle\phi^I(t)\right|\mu^I(t)\left|\phi^I(t)\right\rangle \quad (10)$$

We substitute $\left|\phi^I(t)\right\rangle$ with (8). To distinguish different perturbation orders in the polarization, we can represent it as $P(t) = \sum_n P^{(n)}(t)$, where

$$P^{(n)}(t) = \sum_{m=0}^{n}\left\langle\phi^{(n-m)}(t)\right|\mu^I(t)\left|\phi^{(m)}(t)\right\rangle \quad (11)$$

The perturbations to the state $\left|\phi^{(m)}(t)\right\rangle$ include m integrals over $V(t)$, and $V(t) \sim \sum_{j=1}^{3}\left(E_j(t)e^{-i\omega_j t + i\vec{k}_j\vec{r}} + \text{c.c.}\right)$. Thus, each of the terms in (11) consists of subterms, that are proportional to $\exp\{i\sum_j l_j\vec{k}_j\vec{r}\}$ where $l_j \in [-m, m]$. These subterms are contributions to the intensity of the emission in corresponding directions.

The first non-zero perturbation with directions of emitted light different from the incident light directions $\{k_1, k_2, k_3\}$, is $P^{(3)}(t)$. We'll consider only this perturbation as the strongest one.

III. Application to Logic

To consider the implementation of binary logic let us explore possible evolution paths of the system. Different evolution paths correspond to different propagation directions of the scattered light. We assume that we can detect only in one direction. It allows us to disregard most of the evolution trajectories, as they correspond to other directions.

Those that we are interested in, are presented in Fig. 2, where the nodes represent the states that contribute to the $P^{(3)}$: the left(right) number corresponds to the excitation of a ket(bra) state. The excitation of a ket(bra) state by ith pulse corresponds of the plus(minus) sign before k_i in the emission direction. The relaxation due to the stimulated emission corresponds to the opposite sign. The direction we detect in is the rephasing direction (R) $-k_1 + k_2 + k_3$.

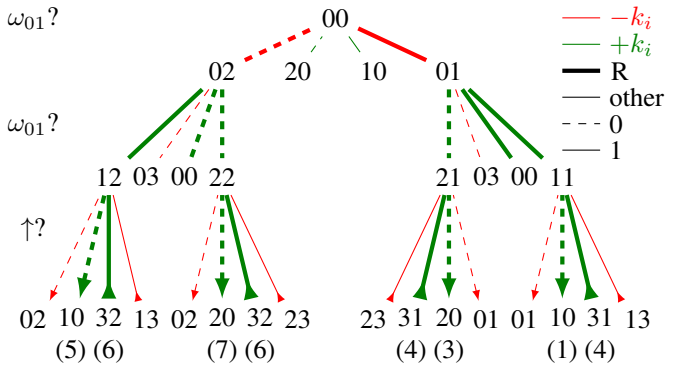

Fig. 2. Diagram of the evolution of the system under the three pulses. The legend is in the upper right corner: green (red) lines correspond to $(-)k_i$, and the lines that correspond to rephasing direction $-k_1 + k_2 + k_3$ are marked as thick. The questions to the left give rise to three binary variables, and the paths that correspond to answer 0(1) are shown with dashed(solid) lines. The numbers in brackets below final states indicate the corresponding positions on the R spectrum Table I.

A. First pulse

The initial state is $|\phi(t_0)\rangle = |0\rangle$. The first excitation corresponds to a term in (11) that includes either $V(t_1)\,|0\rangle$ or $\langle 0|\,V(t_1)$. The operator $V(t_1)$ acting on $|0\rangle$ excites either $|1\rangle$ or $|2\rangle$ (and same for the bra vectors). Thus, there are four possible options for a transition: 01, 10, 02 and 20.

Excitation of 01 and 02 corresponds to $-k_1$, while 10 and 20 contribute $+k_1$ to the total wave-vector. As we are interested only in the direction, that includes $-k_1$, we will not continue the branches of 20 and 10.

Let us define excitation frequency Ω_{exc} as the frequency of the transition induced by the first pulse. If 01 is excited, $\Omega_{exc} = \omega_{01}$, as can be seen from the scheme of the energy levels in Fig. 1, and similarly $\Omega_{exc} = \omega_{02}$ for the excitation of 02 by the first pulse.

B. Second and third pulses

The situation is similar for the second pulse, with two exceptions. First, now we are interested in the transitions corresponding to $+k_2$ (they are shown with thick lines). Second, the system is now not in the ground state, but in a superposition of the excited states $|1\rangle$ and $|2\rangle$, and is evolving under the free Hamiltonian H_0.

The interaction between the pulse and the system depends on the state of the system. Thus by tuning the delay between the pulses, one is able to choose the state in which the system will be at the time of the second pulse, and hence to define the probabilities of different transitions. This is the way to implement a particular logic function.

The trajectories involving 00 state after the second pulse (the ground state bleach, GSB) are not considered in the logic implementation, as their contribution is a constant with respect to the time between the 2nd and the 3rd pulses [5].

The third pulse induces transitions at multiple frequencies. A binary variable corresponding to this transition is linked with a question, whether the interaction with the field induced an

TABLE I
POSSIBLE COMBINATIONS OF THE EMISSION FREQUENCY Ω_{em} AND THE EXCITATION FREQUENCY Ω_{exc}.

Ω_{exc} \ Ω_{em}	ω_{01}	ω_{23}	ω_{02}	ω_{13}
ω_{02}	5	6	7	8
ω_{01}	1	2	3	4

absorption of a photon and excitation of a higher state (shown with arrows pointing up), or it was a stimulated emission that caused relaxation of the system (shown with downwards arrows).

The frequency of the final emission is a frequency of the transition between the bra and ket states in the final node (i.e., the system in a node ij after the third pulse will emit at ω_{ij}). These four values of the emission frequency Ω_{em} together with the two values of the excitation frequency Ω_{exc} present 8 possible combinations. Let us enumerate them as shown in Table I.

C. Introducing logical variables

The 8 possible values of the two frequencies give rise to the three logical variables.

The first transition can happen at one of the two frequencies: ω_{01} and ω_{02}. Therefore the value of the first logical variable corresponds to the question "is the frequency Ω_{exc} equal to ω_{01}"?

Transitions induced by the second pulse happen at all the four frequencies of the system, however each of the paths within R contributions presents a choice between ω_{01} and another frequency. Thus the value of the second logical variable corresponds to the same question "was the transition frequency equal to ω_{01}?"

During the third pulse in each of the paths there is either an absorption or an emission of a photon by a system. The value of the third logical variable corresponds to the question "was there an absorption?"

The transitions corresponding to logical 0 (1) are shown in the diagram Fig. 2 with dashed (solid) lines.

If the three bits corresponding to "ω_{01}?", "ω_{01}?" and "$\uparrow$?" are labeled and ordered as abc, they can be represented with a decimal value $x = 2^0c+2^1b+2^2a$. The logical values (columns 2 to 4), the decimal value x corresponding to them (column 1) and the corresponding points on the spectrum Table I for R direction (5th column) are presented in the Table II. Here we also consider the non-rephasing (NR) direction $k_1 - k_2 + k_3$ (6th column).

A concatenation of Tables I and II give the Table III that shows the correspondence between the decimal value of the input and the excitation and emission frequencies.

The observable $P^{(3)}(t)$, measured at R direction, includes the contributions of different trajectories. The spectrum obtained from a single experiment allows to obtain an evaluation of a logical function for multiple values of its inputs simultaneously. By tuning the time between the second and the third pulses it is possible to choose, what paths will be possible, and thus to choose values of 1 or 0 for different points in the spectrum, thereby encoding different functions.

TABLE II
THE LOGICAL VALUES AND THE POINTS ON THE SPECTRUM (TABLE I) OF REPHASING CONTRIBUTIONS R AND NON-REPHASING CONTRIBUTIONS NR.

x	ω_{01}?	ω_{01}?	$\uparrow$?	R spectrum point	NR spectrum point
0	0	0	0	7	7
1	0	0	1	6	6
2	0	1	0	5	7
3	0	1	1	6	8
4	1	0	0	3	2
5	1	0	1	4	2
6	1	1	0	1	1
7	1	1	1	4	4

TABLE III
CORRESPONDENCE BETWEEN THE COMBINATIONS OF THE EMISSION FREQUENCY Ω_{em} AND THE EXCITATION FREQUENCY Ω_{exc} ON ONE HAND, AND THE INPUTS x OF THE LOGICAL FUNCTIONS.

Ω_{exc} \ Ω_{em}	ω_{01}	ω_{23}	ω_{02}	ω_{13}
ω_{02}	2	1, 3	0	-
ω_{01}	6	-	4	5, 7

Note that not all the functions are possible to encode with the detection in R direction, but only those satisfying $f(100) = f(110)$ and $f(101) = f(111)$. There are two possibilities to realize functions not satisfying these conditions. The first one is to consider several directions: the last column of the Table II shows the relation between the logical variables and the spectrum for the NR direction: the values of the inputs corresponding to the points on the spectra are different. Another way to evaluate more functions is to use the permutations of variables, or to permute the variables with their complements. In the following we restrict ourselves to the latter option.

The value of a function $f(x)$ is equal to 1 (0) in the case when the detected intensity for the pair of frequencies $\Omega_{exc}, \Omega_{em}$ is higher (lower) then some threshold.

IV. ADDER IMPLEMENTATION

A. Logic operations

This section describes operation of addition of (sets of) two numbers a and b with the COPAC device. Their sum is denoted as s:

$$s = a + b \tag{12}$$

Any number a can be represented in binary form as

$$a = a_n a_{n-1} ... a_1 a_0.$$

For example, $3_{dec} = 011_{bin}$. In the following we shall omit the subscripts dec and bin where the representation is clear from the context. Note that if a and b are n-bit numbers, their sum s contains $n + 1$ bit.

The logical operations used in the following are: OR ($a_i + b_i$), AND ($a_i b_i$), EXOR ($a_i \oplus b_i$). They are commutative and associative, AND is distributive over OR and EXOR.

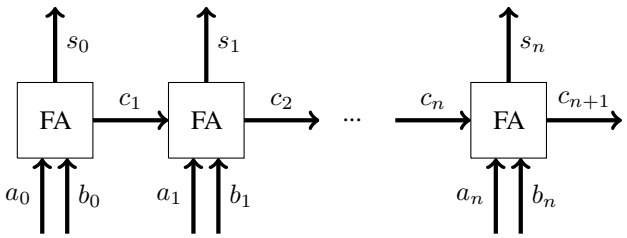

Fig. 3. n-bit adder

TABLE IV
THE TRUTHTABLE FOR THE FA. THE DECIMAL VALUES OF THE INPUT $a_ib_ic_i$ AND OUTPUT $c_{i+1}s_i$ ARE GIVEN BY x AND y RESPECTIVELY.

x	a_i	b_i	c_i	c_{i+1}	s_i	y
0	0	0	0	0	0	0
1	0	0	1	0	1	1
2	0	1	0	0	1	1
3	0	1	1	1	0	2
4	1	0	0	0	1	1
5	1	0	1	1	0	2
6	1	1	0	1	0	2
7	1	1	1	1	1	3

B. Logical n-bit adder

An n-bit adder is a logical circuit that takes two n-bit numbers a and b as inputs and returns $(n+1)$-bit number that represents their sum s. Alternatively: it takes $2n$ single bits as inputs and maps them on $(n+1)$ single-bit output. It can be seen as a sequence of full adders (FA), as in Fig. 3.

FA takes tree bits as inputs: two from the addends (a_i and b_i) and one as a carry out c_i from the addition of lower order bits, and returns two outputs: sum s_i and carry out c_{i+1}, that are calculated according to

$$s_i = a_i \oplus b_i \oplus c_i \tag{13}$$

$$c_{i+1} = a_i b_i + (a_i \oplus b_i)\, c_i \tag{14}$$

$$c_0 = 0 \tag{15}$$

$$s_{n+1} = c_{n+1} \tag{16}$$

Eq. (15) represents the initial condition arising from the fact that there is no carry to take into the first adder. Eq. (16) shows that the $(n+1)$th bit of the result s of the addition of two n-bit numbers a and b is a carry out of the last FA.

The FA has two outputs, s_i and c_{i+1}, that correspond to different logic functions (13) and (14) respectively. We assume that they can be realized by tuning the time between the second and the third pulses to the values of T_s and T_c respectively.

The truth table for the FA is shown as Table IV, representing (13) and (14). The x column presents the decimal value of binary number $x = (a_ib_ic_i)_{dec}$, and the last column gives the decimal value of the binary result of FA calculation $y = (c_{i+1}s_i)_{dec}$.

C. Single bit addition

Building on these premises, let us first present the set of operations required to implement a single FA, that is equivalent to an addition of three single bits. It is done by the following algorithm

1) Find the pair of frequencies $\Omega_{exc}, \Omega_{em}$ corresponding to $a_ib_ic_i$
2) Calculate s_i:
   a) Excite the system with a first pulse at frequency Ω_{exc}
   b) Excite the system with a spectrally broad second pulse
   c) Wait for time T_s between the 2^{nd} and the 3^{rd} pulses
   d) Excite the system with a spectrally broad third pulse
   e) Collect the output at Ω_{em}
   f) Save it as s_i
3) Calculate c_{i+1}:
   a) Repeat 2a.-2b.
   b) Wait for time T_c between the 2^{nd} and the 3^{rd} pulses
   c) Repeat 2d.-2e.
   d) Save the output as c_{i+1}

Let us explore several examples. First, let's assume there is no carry out of the previous addition ($c_i = 0$).

The input of the simplest addition 0+0 ($a_i = 0$, $b_i = 0, x = 0$), according to the Table III, corresponds to the excitation at $\Omega_{exc} = \omega_{02}$ and collection at $\Omega_{em} = \omega_{02}$. As, the value of both functions s_i and c_{i+1} for $x = 0$ is zero, the detected signal will be below the threshold for both waiting times T_s and T_c, thus implementing $s_i(0) = 0, c_{i+1}(0) = 0$.

The addition 1+0 ($a_i = 1$, $b_i = 0, x = 4$) corresponds to the excitation at $\Omega_{exc} = \omega_{01}$ and collection at $\Omega_{em} = \omega_{02}$. When the function s_i (c_{i+1}) is implemented, the detected signal will be above (below) the threshold. Together the two output bits $c_{i+1}s_i = 01_{bin} = 1_{dec}$.

The addition 1+1 ($a_i = 1$, $b_i = 1, x = 6$) corresponds to the excitation at $\Omega_{exc} = \omega_{01}$ and collection at $\Omega_{em} = \omega_{01}$. When the function s_i (c_{i+1}) is implemented, the detected signal will be below (above) the threshold. Together the two output bits $c_{i+1}s_i = 10_{bin} = 2_{dec}$.

If $c_i = 1$, addition 1+1 ($a_i = 1$, $b_i = 1$) now corresponds to x=7 and to the excitation at $\Omega_{exc} = \omega_{01}$ and collection at $\Omega_{em} = \omega_{13}$. For both outputs the detected intensity will be above threshold, thus $a_ib_ic_i = 111_{bin} \Rightarrow c_{i+1}s_i = 11_{bin} = 3_{dec}$.

However, the value $a_ib_ic_i = 101_{bin} = 5_{dec}$ corresponds to the same set of frequencies as $x = 7$. As $c_{i+1}(5) = c_{i+1}(7)$, this is not a problem for the carry out calculation. But for the implementation of the function s_i this will pose a challenge: $s_i(5) = 0$, while $s_i(7) = 1 > s_i(5)$, thus the signal from $x = 7$ makes impossible to measure the absence of signal that should occur for $x = 5$. This can be solved by a permutations of the bits of the input, when such a situation occurs, for the bits where the functions have the same values. The problem arises for $c_{i+1}(1), s_i(3), s_i(5)$, thus the possible permutations to be made are: $001 \to 010$, $011 \to 110$, $101 \to 110$.

D. Parallel single bit addition

To have several parallel calculations, we can exploit quantum superposition. This can be done in twofold way:

- by detection at several frequencies
- by excitation at several frequencies

However, in order to be able to distinguish between outputs from different inputs, only such values can be evaluated at parallel, that correspond to different emission frequencies.

The algorithm of evaluation in this case should be modified:

1) Find the pairs of frequencies $(\Omega_{exc}, \Omega^j_{em}), j \in [1,k], k \leq 3$ corresponding to $(a_i b_i c_i)^j$
2) Calculate s_i:
   a) Excite the system with a first pulse at frequency Ω_{exc}[5]
   b) Excite the system with a spectrally broad second pulse
   c) Wait for time T_s between the 2^{nd} and the 3^{rd} pulses
   d) Excite the system with a spectrally broad third pulse
   e) Collect the output at $\Omega^1_{em}, \Omega^2_{em}, ..., \Omega^k_{em}$
   f) Save it as $s^1_i, s^2_i, ..., s^k_i$
3) Calculate c_{i+1}:
   a) Repeat 2a.-2b.
   b) Wait for time T_c between the 2^{nd} and the 3^{rd} pulses
   c) Repeat 2d.-2e.
   d) Save the output as $c^1_{i+1}, c^2_{i+1}, ..., c^k_{i+1}$

For example, one can compute 1+0+0, 1+1+0 and 1+1+1 at the same time. The excitation frequency is ω_{02}, and the results of detection at ω_{02}, ω_{01}, ω_{23} are written in $s_i(100), s_i(110), s_i(111)$, and the same for c_{i+1}.

Thus, a parallel computation of up to three sums of three two-bit variables can be performed by two calls to the COPAC device. One call takes $\lesssim 1\mu$s (**is this true?**), which is comparable with clock rates of modern computers. Thus, potentially, calculations with the COPAC machine can outperform the state-of-art technologies. When more than three sums need to be computed, they must be divided into groups of sums that are possible to evaluate at a single call.

E. Parallel n-bit addition

The optimal way to implement a n-bit adder would be to compute first all the c_{i+1} values and store them, and then reuse them to compute the s_i. A new computed value of s_i would be stored in place of c_i. The computation of multiple s_i at one call is optimal because it allows broader use of parallel computation.

As an example, let us consider three sums: 6+6, 2+1, 2+5. In binary: 110+110, 010+001, 010+101. One can notice, that the first two bits of the two last sums coincide, which allows to reduce number of calculations.

First we consequently evaluate c_i according to the algorithm above. For the first bit $\Omega_{exc} = \omega_{02}$, $[\Omega^1_{em}, \Omega^2_{em}, \Omega^3_{em}] = [\omega_{02}, \omega_{01}, \omega_{01}]$, and the results are $[c^1_1, c^2_1, c^3_1] = [0,0,0]$. For the second bit $\Omega_{exc} = \omega_{01}$, $[\Omega^1_{em}, \Omega^2_{em}, \Omega^3_{em}] = [\omega_{01}, \omega_{02}, \omega_{02}]$, and the results are $[c^1_2, c^2_2, c^3_2] = [1,0,0]$. For the third bit we need two calls: $\Omega_{exc} = \omega_{01}$, $\Omega^1_{em} = \omega_{13}$, $c^1_3 = 1$ and $\Omega_{exc} = \omega_{02}$, $[\Omega^2_{em}, \Omega^3_{em}] = [\omega_{02}, \omega_{01}]$, $[c^2_3, c^3_3] = [0,0]$.

Then we have 9 entries to evaluate s_i on. First bit: 000, 010, 010; second bit: 110, 100, 100; third bit: 111, 000, 010. They can be evaluated in two calls:

1) $\Omega_{exc} = \omega_{02}$, $[\Omega^1_{em}, \Omega^2_{em}] = [\omega_{02}, \omega_{01}]$, and the results are $s^1_0, s^2_2, s^2_0 = 0$ (evaluated at ω_{02}), $s^3_0, s^3_2 = 1$ (evaluated at ω_{01}).
2) $\Omega_{exc} = \omega_{01}$, $[\Omega^1_{em}, \Omega^2_{em}, \Omega^3_{em}] = [\omega_{01}, \omega_{02}, \omega_{13}]$, and the results are $s^1_1 = 0$,$s^2_1, s^3_1 = 1$, $s^1_2 = 1$ at the respective frequencies.

Thus, if the delay of a single gate is D, the total delay in this example is $6D$ for three 3-but additions, that in a classical ripple-carry adder would take $21D'$, where the single gate time may differ.

V. Summary

In this paper we presented the principles behind a device developed under COPAC project and able to evaluate a logical function for multiple values of inputs in parallel. The algorithm to implement a n-bit adder with a COPAC machine was suggested, showing that the machine provides the speedup due to the possibility to compute several additions in parallel.

In the paper we focused on a quantum system with 4 eigenstates, connected as in Fig. 1. However, different configurations can be engineered, providing more input variables and more possibilities for parallel computation.

[5]One can also excite at both excitation frequencies ω_{02} and ω_{01} (or with a broad pulse), but with prudence, avoiding the situations when the signal for different Ω_{exc} and same Ω_{em} overshadows the absence of signal that we are looking for.

References

[1] Susan Stepney, Steen Rasmussen, and Martyn Amos. *Computational Matter*. Springer, 2018.

[2] F Remacle and RD Levine. Towards a molecular logic machine. *The Journal of Chemical Physics*, 114(23):10239–10246, 2001.

[3] Françoise Remacle, Rainer Weinkauf, and Raphael D Levine. Molecule-based photonically switched half and full adder. *The Journal of Physical Chemistry A*, 110(1):177–184, 2006.

[4] Barbara Fresch, Dawit Hiluf, Elisabetta Collini, RD Levine, and Françoise Remacle. Molecular decision trees realized by ultrafast electronic spectroscopy. *Proceedings of the National Academy of Sciences*, 110(43):17183–17188, 2013.

[5] Barbara Fresch, Marco Cipolloni, Tian-Min Yan, Elisabetta Collini, RD Levine, and Françoise Remacle. Parallel and multivalued logic by the two-dimensional photon-echo response of a rhodamine–dna complex. *The journal of physical chemistry letters*, 6(9):1714–1718, 2015.

[6] Ron Orbach, Fuan Wang, Oleg Lioubashevski, RD Levine, Francoise Remacle, and Itamar Willner. A full-adder based on reconfigurable dna-hairpin inputs and dnazyme computing modules. *Chemical Science*, 5(9):3381–3387, 2014.

[7] Elisabetta Fanizza, Carmine Urso, Vita Pinto, Antonio Cardone, Roberta Ragni, Nicoletta Depalo, M Lucia Curri, Angela Agostiano, Gianluca M Farinola, and Marinella Striccoli. Single white light emitting hybrid nanoarchitectures based on functionalized quantum dots. *Journal of Materials Chemistry C*, 2(27):5286–5291, 2014.

[8] Oren Ben Dor, Noam Morali, Shira Yochelis, Lech Tomasz Baczewski, and Yossi Paltiel. Local light-induced magnetization using nanodots and chiral molecules. *Nano letters*, 14(11):6042–6049, 2014.

[9] Eyal Cohen, Michael Gruber, Elisabet Romero, Shira Yochelis, Rienk van Grondelle, and Yossi Paltiel. Properties of self-assembled hybrid organic molecule/quantum dot multilayered structures. *The Journal of Physical Chemistry C*, 118(44):25725–25730, 2014.

[10] Feynman grand prize : https://foresight.org/grandprize.1.html.

[11] Tian-Min Yan, Barbara Fresch, RD Levine, and Francoise Remacle. Information processing in parallel through directionally resolved molecular polarization components in coherent multidimensional spectroscopy. *The Journal of chemical physics*, 143(6):064106, 2015.

[12] Shaul Mukamel. *Principles of nonlinear optical spectroscopy*, volume 29. Oxford university press New York, 1995.